JOURNAL OF APPLIED PHYSICS **117**, 193908 (2015)

Giant volume magnetostriction in the Y_2Fe_{17} single crystal at room temperature

S. A. Nikitin,[1,a)] N. Yu. Pankratov,[1] A. I. Smarzhevskaya,[1] G. A. Politova,[1] Yu. G. Pastushenkov,[2,b)] K. P. Skokov,[2] and A. del Moral[3]
[1]*Physics Faculty, Lomonosov Moscow State University, Moscow 119992, Russia*
[2]*Physics Faculty, Tver State University, 170100 Tver, Russia*
[3]*Laboratorio de Magnetismo de Slidos, Departamento de Fisica de Materia Condensada and Instituto de Ciencia de Materiales de Aragn, Facultad de Ciencias, Universidad de Zaragoza-C.S.I.C, E-50009 Zaragoza, Spain*

(Received 3 October 2014; accepted 19 April 2015; published online 20 May 2015)

An investigation of the Y_2Fe_{17} compound belonging to the class of intermetallic alloys of rare-earth and 3d-transition metals is presented. The magnetization, magnetostriction, and thermal expansion of the Y_2Fe_{17} single crystal were studied. The forced magnetostriction and magnetostriction constants were investigated in the temperature range of the magnetic ordering close to the room temperature. The giant field induced volume magnetostriction was discovered in the room temperature region in the magnetic field up to 1.2 T. The contributions of both anisotropic single-ion and isotropic pair exchange interactions to the volume magnetostriction and magnetostriction constants were determined. The experimental results were interpreted within the framework of the Standard Theory of Magnetostriction and the Landau thermodynamic theory. It was found out that the giant values of the volume magnetostriction were caused by the strong dependence of the 3d-electron Coulomb charge repulsion on the deformations and width of the 3d-electron energy band.
 [http://dx.doi.org/10.1063/1.4919593]

I. INTRODUCTION

The magnetostriction is the occurrence of the mechanical deformation variations of magnetic samples due to the changes in the magnetization degree or in the magnetization direction. The microscopic origin of the magnetostriction involves the interaction of the orbital atomic moment with the electric charges in the crystalline lattice (the crystal field). The magnetostriction is also observed when a magnetic field is applied to a magnetized sample; in this case, it is called forced magnetostriction.[1] The forced magnetization contributes to a number of effects such as the forced magnetostriction, thermal expansions, and magnetocaloric effect.[1]

The forced magnetostriction of intermetallic compounds of 3d-transition and rare-earth metals (REM) was investigated in two temperature regions. The first temperature region is close to the temperature of magnetic phase transition (T_C),[1] and the second one is significantly lower than T_C in a strong magnetic field.[2–4] It is known that the forced magnetostriction is insignificant at low temperatures ($T \ll T_C$); however, it is large close to T_C.[1,3]

The intermetallic compounds of 4f- and 3d-transition metals form an important class of materials with giant magnetostriction. It is possible to achieve giant values of magnetostriction in some compounds based on the REM, which is very important for practical application.[6,7] The theory of magnetostriction of 3d–4f intermetallics has been reported in a number of scientific papers;[8,9] however, no research has been conducted on the forced magnetostriction contribution near the Curie temperature. The R_2Fe_{17} compounds are particularly useful for this kind of investigations.

The R_2Fe_{17} compounds are regarded as two-sublattice magnetics with the magnetic sublattices of the REM and iron. Both positive and negative exchange interactions occur in the iron sublattice,[10] which in some cases causes the appearance of the noncollinear antiferromagnetic structure[11,12] and invar behaviour of the thermal expansion.[13–16] It is known that extremely high values of the ΔM effect (the magnetization change due to the pressure change)[17,18] and the forced magnetostriction[19–21] are caused by the strong dependence of the exchange interaction and the width of the 3d-electron energy band on the unit cell volume and the interatomic distance. The high values of the ΔM effect and the magnetostriction are explained by the unit cell deformations due to the magnetization increase at the forced magnetization. It is known that the R_2Fe_{17} (R = Dy-Lu, Y) compounds crystallize into a hexagonal Th_2Ni_{17}-type structure with $P6_3/mmc$ space group.[22] The unit cell contains two formula units with 34 atoms of Fe that occupy four inequivalent positions. The mentioned data concerning the magnetoelastic properties of the R_2Fe_{17} compounds indicate that these compounds show some interesting physical properties and they are excellent model objects for analyzing physics of the magnetic phenomena. However, the important physical properties of the R_2Fe_{17} compounds, including magnetoelastic characteristics (the magnetostriction constants, volume magnetostriction, and dependence of the volume magnetostriction on the magnetization) in the temperature region close to the magnetic phase transition, have not been investigated thoroughly. At the same time, the effects connected with the forced magnetization in this temperature region can be

a)nikitin@phys.msu.ru
b)yupast@mail.ru

clearly observed because the forced magnetization in the given case substantially contributes into the magnetization process. The peculiarities of the magnetoelastic effect in the R_2Fe_{17} compounds in comparison with classic ferromagnet occur at the forced magnetization due to the coexistence of both positive and negative exchange interactions.[1,4] The concepts of dumbbell pairs of iron atoms and 3d-band model help explain different characteristics of these compounds.[4,23] Furthermore, it is necessary to obtain new data on magnetoelastic and magnetic characteristics of single crystals of these compounds.

The aim of this paper is to thoroughly investigate the magnetization, magnetostriction, and thermal expansion of the Y_2Fe_{17} single crystal in the Curie temperature region and also to determine the dependences of the magnetostriction on the magnetization, the magnetostriction constants on the temperature, and the value of exchange interaction on the unit cell volume. Special attention is given to the study of the field induced volume magnetostriction, which is connected with the unit cell deformation dependences on the width of 3d-electron energy band and the exchange interactions.[4,20] This kind of magnetostriction is clearly noticeable at the Curie temperature (T_C). The magnetostriction characteristics in the Curie temperature region are also discussed in accordance with the Landau theory[1,24] and the Standard Theory of Magnetostriction (STM).[4]

In this work, the rare-earth ions were replaced by yttrium. This metal has a very small atomic magnetic moment ($\sim 0.4\,\mu_B$), whereas the local magnetic moments of the Fe atoms in different crystallographic positions have the values of 1.9–2.4 μ_B.[25] Yttrium is a Pauli paramagnet and its ions are located in the crystal lattice as three-valence ions, which is similar to rare-earth ions of the yttrium sub-group. At the same time, the ion radius of yttrium is close to the radius of rare-earth ions.[26] Therefore, the studying of the Y_2Fe_{17} single crystal magnetism provides important information on the Fe sublattice for the whole class of the R_2Fe_{17} compounds.

II. EXPERIMENTAL TECHNIQUES AND SAMPLE PREPARATION

The initial Y_2Fe_{17} alloy was produced by the induction melting method from 99.9% pure yttrium and 99.998% pure iron in the atmosphere of pure argon in the alumina crucible. The ingot was cooled down (10 K/min) to provide conditions appropriate to grow large single crystal grains. It was found out that at the annealing at 1800 K with the subsequent cooling to 1500 K followed by slow cooling to 1400 K for 3–8 h, it is possible to obtain single crystals of the main phase. The large single crystal grains (up to 200 mg) were separated from the ingot.

The phase composition investigation was carried out by the methods of optical metallography, X-ray diffraction phase analysis, and scattering X-ray spectroscopy. The quantitative phase analysis was conducted by the Rietveld method with the PowderCell program using the data of X-ray phase analysis. The X-ray data were obtained by the diffractometer DRON-8 (Fe K_α radiation). It was shown that the crystal structure of the Y_2Fe_{17} alloy is single phased with hexagonal crystal lattice of the Th_2Ni_{17}-type (space group D^4_{6h} or $P6_3/mmc$) and the following lattice parameters: $a = 0.8467$ nm and $c = 0.8318$ nm.

The magnetization was carried out by the SQUID magnetometer (Quantum Design Magnetic Property Measurement System (MPMS) 5-S) in magnetic fields up to 3 T in the temperature range of 5–350 K.

For the magnetostriction measurements, single crystals were oriented by the Laue back-reflection method and were cut in the form of a disk with its plane containing two out of three main crystallographic directions (a, b, and c). To remove the strain from the surface of the samples, electrochemical polishing was carried out.

The magnetostriction and thermal expansion were obtained by the strain gauge technique with the compensation of strain gauge magnetic resistance.[4,5] The linear size of the strain gauge was ~5 mm, and the resistance was 120 Ω. The first gauge was glued to the surface of the sample and the second one was glued to the quartz plate. Both gauges were connected to the opposite arms of the Wheatstone bridge to compensate magnetic resistance. The accuracy of measurements of magnetostriction and thermal expansion was ~3%. The temperature was detected by the differential copper-constantan thermocouple with its signal measured by a microvoltmeter. The accuracy of temperature determination was 0.1 K. The temperature and field dependencies of both longitudinal and transversal magnetostriction were studied in the temperature range of 100–350 K in fields up to 1.2 T.

III. EXPERIMENTAL RESULTS

A. Magnetization

The magnetization (M) along the main crystallographic directions of the Y_2Fe_{17} single crystal was studied in the temperature region of 5–350 K in magnetic fields up to 3 T. Fig. 1(a) shows the temperature dependencies of the magnetization $M(T)$ along the easy magnetization axis (crystallographic direction a in the basal plane). It is seen that all curves at $H \parallel a$ are characterized by the monotonous decrease in magnetization with the increase in temperature.

Fig. 2 shows an abrupt decrease of magnetization in a low field of $\mu_0 H = 0.4$ mT along easy axis in the temperature range of 315–330 K, which arises during the transition from the ferromagnetic to the paramagnetic state. The Curie temperature ($T_C = 324$ K) was determined as the inflection point on the $M(T)$ curve in the field $\mu_0 H = 0.4$ mT.

Fig. 1(b) displays the temperature dependencies of the magnetization along the hard magnetization axis (crystallographic direction c). It is seen that the curves at $H \parallel c$ are characterized by the maximums at $T < T_C$. It is important to notice that the maximum values on $M(T)$ curves are observed in relatively strong fields $\mu_0 H \simeq 1$ T not only close to T_C but also at lower temperatures—for example, at 20 K lower than T_C. Therefore, these values cannot be explained by the Hopkinson effect, which is observed in ferromagnetic materials close to T_C only in the low field region.

The temperatures of the maximums are shifting towards lower values with the increase of the magnetic field. Similar behaviour of the magnetization along the hard magnetization

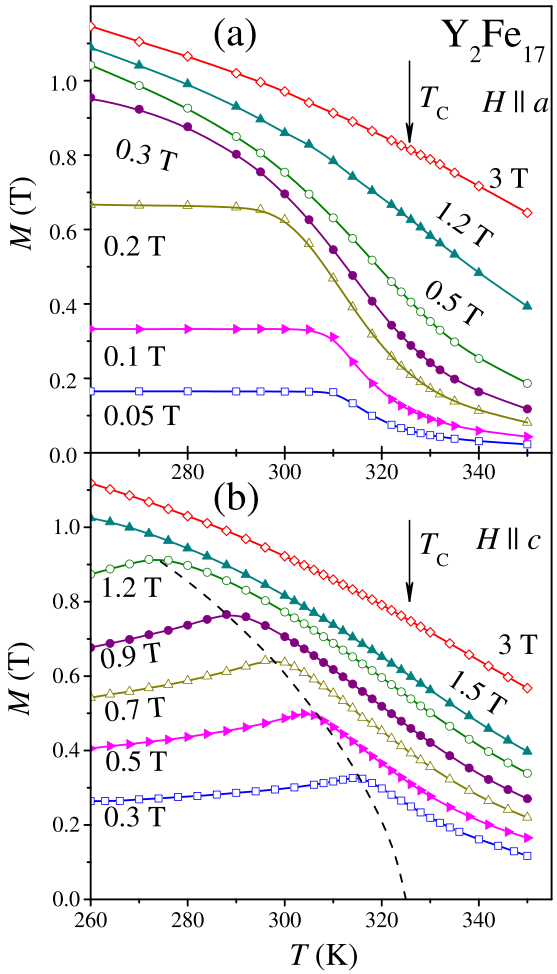

FIG. 1. Temperature dependencies of magnetization of Y_2Fe_{17} single crystal along both *a* (a) and *c* (b) crystallographic directions in different magnetic fields.

axis has been observed in other rare-earth magnets.[27] This phenomenon has been explained by low-symmetry and high-symmetry magnetic phases, which existence depends on the value of the magnetic field $H \parallel c$.[27] The low-symmetry phase is observed in a magnetic field with a value less than critical (H_{cr}). This phase is characterized by the coexistence of both components of the magnetization vector (along and perpendicularly to the c axis). Therefore, in this phase, the magnetization vector is not parallel to the field direction and the c axis. The high-symmetry phase with $M \parallel c$ (the magnetization vector is aligned to the field $H \parallel c$) exists at $H > H_{cr}$. The maximum on the $M(T)$ curve occurs at the temperature of transition from the low-symmetry phase to the high-symmetry one. The dotted curve in Fig. 1(b) shows the border that separates the high-symmetry and low-symmetry phases at $H \parallel c$. The magnetization significantly decreases in a low field at $T > T_C$ (Fig. 2), which indicates that there are no extraneous phases in the sample. However, in strong magnetic fields higher than 0.3 T, magnetization decreases relatively slowly at $T > T_C$, which can be explained by intensive paraprocess both close to T_C and at $T > T_C$.

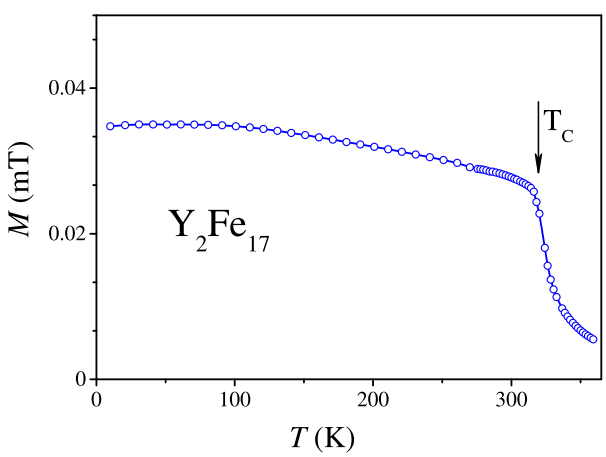

FIG. 2. Temperature dependence of the magnetization of the Y_2Fe_{17} compound along easy axis *a* in the magnetic field $\mu_0 H = 0.4$ mT.

B. Magnetostriction

The magnetostriction value was determined with regard to the direction of the magnetic field and the direction of deformation. Since the strain gauge and the magnetic field were oriented along main crystallographic directions, two indexes were used to designate the magnetostriction. The first index is the direction of the applied field and the second one is the direction of the magnetostriction measurement.

The temperature dependencies of longitudinal and perpendicular magnetostrictions λ_{cc}, λ_{ca}, λ_{aa}, and λ_{ac} are shown in Fig. 3. Here, both λ_{ca} and λ_{aa} are the strains along the *a*-axis in a field along and perpendicular to the *c*-axis, respectively. And both λ_{cc} and λ_{ac} are the strains along hexagonal axis *c* in a magnetic field along and perpendicular to the *c*-axis, respectively. Experimental points were obtained from magnetostriction field dependencies considering magnetostriction measurements that were carried out starting with point $\lambda = 0$. It is seen that the maximum of the magnetostriction is observed near T_C. These diffused maximums on the temperature dependencies of the magnetostriction in the T_C region were explained by the strong dispersion of the exchange integrals due to the coexistence of both positive and negative exchange interactions. Therefore, both the magnetostriction and magnetization data indicate the temperature of magnetic phase transition "paramagnetism-ferromagnetism" at $T_C = 324$ K.

In the region of magnetic phase transition ($T > 250$ K), the values of magnetostrictions λ_{ca}, λ_{cc}, λ_{aa}, and λ_{ac} are positive. The magnetostrictions reach their maximums at T_C (see Fig. 3). The maximum values of the magnetostrictions are different. For example, $\lambda_{ca} = 85 \times 10^{-6}$, $\lambda_{ac} = 155 \times 10^{-6}$, $\lambda_{aa} = 105 \times 10^{-6}$, and $\lambda_{cc} = 120 \times 10^{-6}$ in the field of 1.2 T. The magnetostriction close to T_C is forced[4] for $H \parallel a$ (easy magnetization axis). The values of λ_{aa}, λ_{ca}, λ_{ac}, and λ_{cc} maximums increase together with the magnetic field growth as the result of the forced magnetization in the magnetic phase transition region.

The field dependencies of λ_{aa}, λ_{ca}, λ_{ac}, and λ_{cc} magnetostrictions at the Curie temperature ($T_C = 324$ K) are shown in Fig. 4. Figs. 3 and 4 indicate that the magnetostrictions are positive at the "ferromagnetism-paramagnetism" phase transition and increase together with the growth of the applied

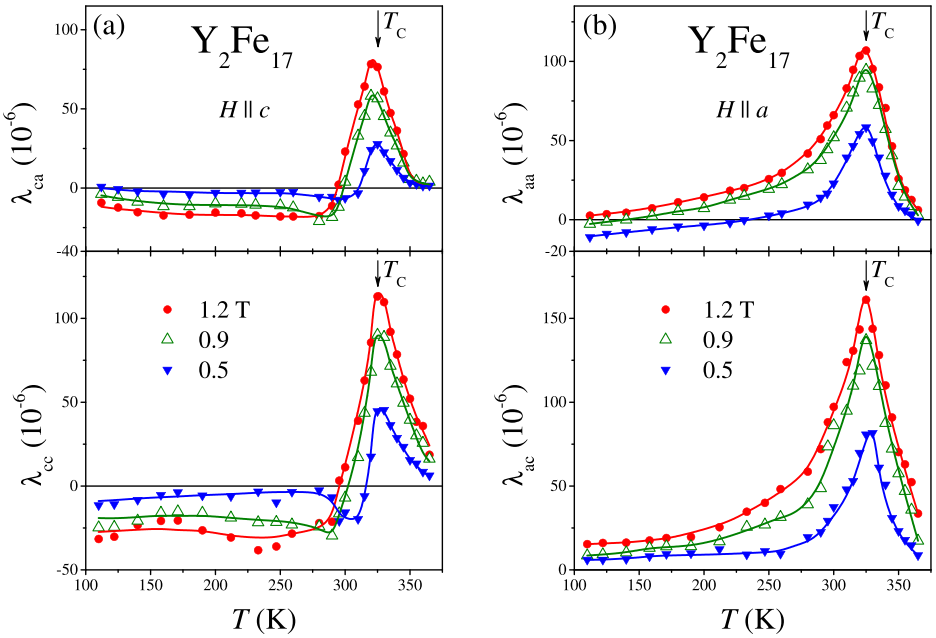

FIG. 3. Temperature dependencies of λ_{aa}, λ_{ca}, λ_{ac}, and λ_{cc} magnetostrictions in magnetic fields of 0.5, 0.9, and 1.2 T along the hexagonal c axis (a) and a axis (b).

magnetic field. The speed of the increase is not the same for different crystallographic and magnetic field directions. Therefore, the anisotropic change of the sample volume occurs due to the forced magnetization.

The magnetostriction saturation at Curie temperature $T_C = 324$ K is not observed. It is known that the saturation of magnetostriction is observed for the processes of rotation of magnetization vectors.[1,4] Therefore, the forced magnetostriction is responsible for the volume magnetostriction near T_C in the Y_2Fe_{17} compound.

We should emphasize that the forced magnetostriction in the Y_2Fe_{17} compound is quite large in moderate magnetic fields close to the Curie temperature. Both longitudinal and transversal magnetostrictions close to T_C are positive and demonstrate high values.

These data clearly indicate that the volume expansion occurs under the influence of the magnetic field. The above-mentioned data indicate that the volume change makes the largest contribution to the magnetostriction close to T_C, which means that large field induced volume magnetostriction occurs in this region.

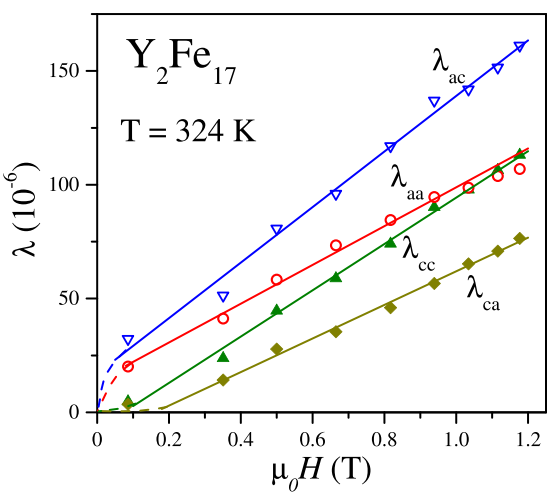

FIG. 4. Field dependencies of λ_{ac}, λ_{ca}, λ_{aa}, and λ_{cc} magnetostrictions at $T_C = 324$ K.

It is noticeable that the $\lambda_{aa}(T)$ and $\lambda_{ac}(T)$ curves (see Fig. 3) are almost symmetrical close to T_C, while the $\lambda_{ca}(T)$ and $\lambda_{cc}(T)$ curves are asymmetric (see Fig. 3) and have minima at T below T_C. The asymmetry of these curves is explained by the complicated nature of the magnetization process along the hard magnetization axis in the anisotropic ferromagnet in the field $H \parallel c$ at $H < H_{cr}$ and $T < T_C$.[27] In this case, the increase of magnetization occurs due to both the forced magnetization and magnetization vector rotation from the basal plane (easy magnetization plane) to the direction of the magnetic field ($H \parallel c$). The negative contribution to the magnetostriction λ_{ca} and λ_{cc} occurs due to the magnetization vector rotation to the direction of hard magnetization axis under the magnetic field $H \parallel c$ that leads to the presence of the minimums on the λ_{ca} and λ_{cc} temperature dependences at $T < T_C$.

C. Thermal expansion

Our data of thermal expansion along the hexagonal axis c $(\Delta\ell/\ell)_c$ and the a-axis in the basal plane $(\Delta\ell/\ell)_a$ obtained by the direct measurements in the temperature range of 100–350 K are shown in Fig. 5 as triangles. For comparison purposes, the thermal expansion at the temperatures up to 750 K calculated according to the X-ray analysis data[15,16] is presented on the same diagrams as filled circles.

It is seen that the thermal expansion detected by the direct measurements and calculated from the indirect measurements coincide precisely in the temperature range of 100–350 K. At the temperatures higher than the Debye temperature (T_D), the thermal expansion has a linear behaviour that allows to extract the phonon contribution $(\Delta\ell/\ell)_{ph}$ using the Debye theory with two parameters (inclination of the line and T_D) taking into account the value of the Debye temperature $T_D = 440$ K.[15] The phonon contributions are shown in Fig. 5 by continuous lines. The spontaneous magnetostrictions along the axis c $\Lambda_c(T)$ and in the basal plane $\Lambda_a(T)$

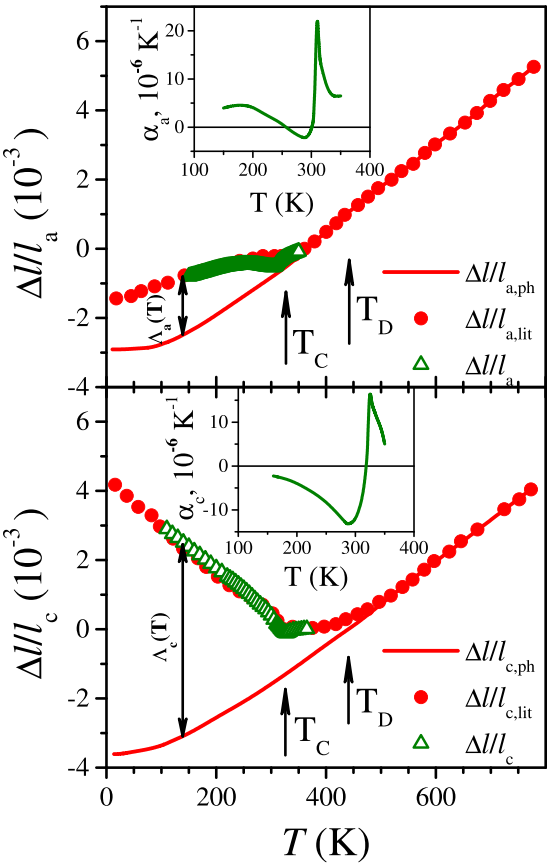

FIG. 5. Temperature dependencies of thermal expansion along the crystallographic directions *a* and *c*. Inset: The thermal expansion coefficients vs temperature along crystallographic directions *a* and *c*.

were found by subtracting $(\Delta\ell/\ell)_{ph}$ from the experimental values of the thermal expansion $(\Delta\ell/\ell)$.

Fig. 5 shows the contributions $\Lambda_c(T)$ and $\Lambda_a(T)$ along $(\Delta\ell/\ell)_{ph}$ considerably change the temperature dependences of the thermal expansion due to their higher values. It should be noticed that the linear size along the axis *c* abnormally increases at cooling below T_C and does not decrease.

The coefficients of thermal expansion (γ_a and γ_c) were found by differentiating the curves of thermal expansion $(\Delta\ell/\ell)_a(T)$ and $(\Delta\ell/\ell)_c(T)$ with the temperature

$$\gamma_{a,c}(T) = \frac{d(\Delta\ell/\ell)_{a,c}}{dT}. \quad (1)$$

The temperature dependencies of thermal expansion coefficients along the hexagonal axis *c* (γ_c) and in the basal plane (γ_a) are shown on the insertions in Fig. 5. The coefficients of thermal expansion have the λ-type temperature dependences close to T_C. Some peculiarities in their behaviour are also seen in the temperature region above T_C. They are the sum of two contributions: an expansion due to the stimulation of the phonons (γ_{ph}) and the magnetostrictive contribution. To explain the abnormal behaviour of (γ_c) and (γ_a), we should consider that $\gamma_{ph} > 0$ according to the Debye theory and the experimental data for the materials without a spontaneous magnetic moment. At some temperatures close to T_C, the positive contribution due to the stimulation of the phonons and the negative magnetostrictive contribution compensate each other, which causes zero values of the thermal expansion coefficient (it is also typical for the invar Fe-Ni alloys).[4] At the temperatures below T_C, the negative magnetostrictive contribution is dominant, which causes the negative values of the γ_c and γ_a coefficients. It is important to notice that the thermal expansion anisotropy is observed: the (γ_a) and (γ_c) coefficients (along *a* and *c* axes) are significantly different.

IV. DISCUSSIONS

A. Calculation of volume magnetostriction and magnetostriction constants within the framework of phenomenological approach

It is well known that in the region of the second order phase transition from the ferromagnetic to paramagnetic state, the orthorhombic distortion and the shear deformations may be disregarded.[4] This conclusion is confirmed by the received experimental results, according to which the magnetostrictions along both *a* and *b* axes in the basal plane (within the limits of possible experimental error ~3%) practically coincide in the temperature range of 200–350 K.[20]

Without considering the orthorhombic distortion and the shear deformations as both of them are not observed in the investigated temperature range, the magnetostrictive deformation can be written according to the STM[4,28]

$$\lambda(\alpha_z,\beta_z) = \frac{1}{3}\lambda_{11}^{\alpha} + 2\lambda_{21}^{\alpha}\left(\beta_z^2 - \frac{1}{3}\right) + \frac{1}{2\sqrt{3}}\lambda_{21}^{\alpha}\left(\alpha_z^2 - \frac{1}{3}\right) + \sqrt{3}\lambda_{22}^{\alpha}\left(\alpha_z^2 - \frac{1}{3}\right)\left(\beta_z^2 - \frac{1}{3}\right), \quad (2)$$

where α_z and β_z are the directing cosines of the magnetization vector *M* and the deformation direction, correspondingly; the quantities of $\lambda_{i,j}^{\alpha}$ as the functions of temperature and applied magnetic field play the role of phenomenological magnetostriction constants.[28–30] On the one hand, the magnetostriction constants λ_{11}^{α} and λ_{21}^{α} are determined by isotropic pair exchange and pseudodipole interactions of two magnetic ions. On the other hand, λ_{12}^{α} and λ_{22}^{α} are determined by anisotropic interaction of the magnetic ion with the crystal field, which is created by the surrounding ions of the crystal lattice. Exchange interactions make an isotropic contribution to the magnetostrictive deformation, which does not depend on the directing cosines of the magnetization vector *M*. At the same time, the single-ion interactions make anisotropic contributions depending on the direction of the magnetization vector.

The volume magnetostriction as a function of variables (*T*, *H*) is presented as[28]

$$\omega(T,H) = \lambda_{11}^{\alpha} + \frac{\sqrt{3}}{2}\lambda_{12}^{\alpha}\left(\alpha_z^2 - \frac{1}{3}\right). \quad (3)$$

From (3), it is possible to calculate the volume magnetostrictions ω_a ($H \parallel a$) and ω_c ($H \parallel c$).[28] In case when the external magnetic field *H* exceeds the anisotropy field (thereby, vector *M* is parallel to the direction of *H*), from (2) and (3) we obtain

$$\omega_a = 2\lambda_{aa} + \lambda_{ac} = \lambda_{11}^{\alpha} - \frac{1}{2\sqrt{3}}\lambda_{12}^{\alpha}, \quad (4)$$

$$\omega_c = 2\lambda_{ca} + \lambda_{cc} = \lambda_{11}^{\alpha} + \frac{1}{\sqrt{3}}\lambda_{12}^{\alpha}. \quad (5)$$

Thereby, the field induced volume magnetostriction is anisotropic relatively to the direction of the applied field H, as a result of the single-ion λ_{12}^{α} contribution.

It is worth noting that the axis ratio c/a of the lattice parameters also changes simultaneously with the volume change. For $(H \parallel a)$ from (2) it is as follows:

$$\lambda_{ac} - \lambda_{aa} = 2\left(\lambda_{21}^{\alpha} - \frac{1}{2\sqrt{3}}\lambda_{22}^{\alpha}\right). \quad (6)$$

For $(H \parallel c)$, it is as follows:

$$\lambda_{cc} - \lambda_{ca} = 2\left(\lambda_{21}^{\alpha} + \frac{1}{\sqrt{3}}\lambda_{22}^{\alpha}\right). \quad (7)$$

Fig. 6 shows the temperature dependencies of the field induced volume magnetostrictions ω_a and ω_c calculated by Eqs. (4) and (5) using the experimental values of the magnetostrictions λ_{ca}, λ_{aa}, λ_{ac}, and λ_{cc}. It is seen that ω_a and ω_c have the giant magnitude close to the Curie temperature: $\omega_a = 360 \times 10^{-6}$ and $\omega_c = 250 \times 10^{-6}$ in the field $\mu_0 H = 1.2$ T. As expected, the ω increased together with the field as in this case the forced magnetostriction was dominant (the forced magnetostriction increases linearly with the field).

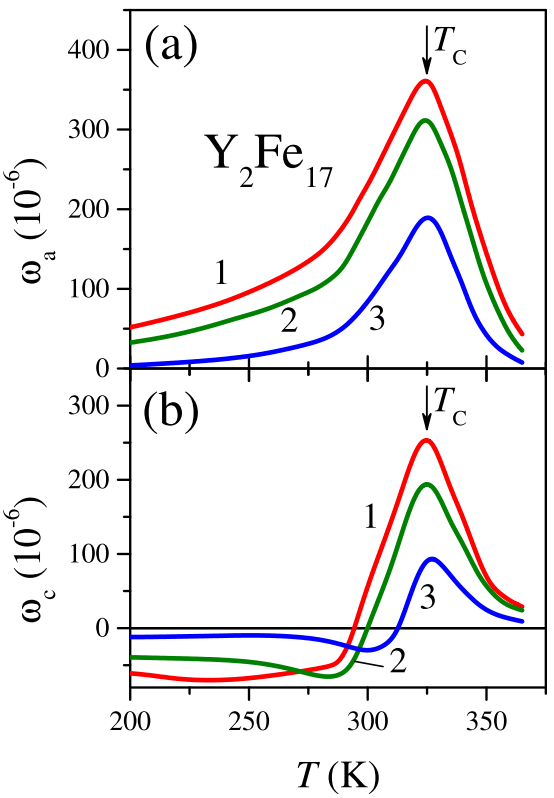

FIG. 6. Temperature dependencies of the field induced volume magnetostriction ω_a and ω_c in different magnetic fields: 1–1.2 T, 2–0.9 T, and 3–0.5 T.

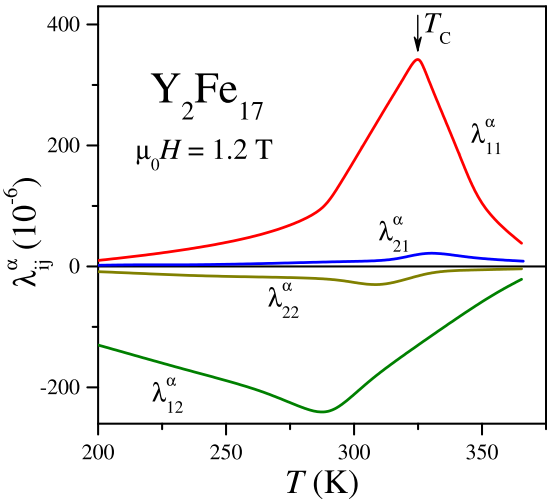

FIG. 7. Temperature dependencies of the magnetostriction constants λ_{11}^{α}, λ_{12}^{α}, λ_{21}^{α}, and λ_{22}^{α} in the magnetic field of 1.2 T.

Using the experimental data on magnetostrictions, the contributions of a crystal field to the axis ratio c/a described by the magnetostriction constants λ_{21}^{α} and λ_{22}^{α} were calculated by (6) and (7). The temperature dependencies of the magnetostriction constants $\lambda_{i,j}^{\alpha}(T,H)$ $(i,j = 1,2)$ in the field $\mu_0 H = 1.2$ T are shown in Fig. 7. It was found that $\lambda_{11}^{\alpha} = 326 \times 10^{-6}$, $\lambda_{12}^{\alpha} = -238 \times 10^{-6}$, $\lambda_{21}^{\alpha} = 16 \times 10^{-6}$, and $\lambda_{22}^{\alpha} = -26 \times 10^{-6}$ at T_C in the magnetic field of 1.2 T. It is seen that near T_C, the magnetostriction constants λ_{11}^{α} and λ_{12}^{α} are significantly higher than λ_{21}^{α} and λ_{22}^{α}.

The maximum on the curves λ_{11}^{α} and λ_{21}^{α} is observed at $T_C = 324$ K, and at the same time for λ_{12}^{α} and λ_{22}^{α}, the maximums are shifted to lower temperatures. This behaviour is caused by the negative contribution into the magnetostriction from the processes of magnetization vector rotation in the low-symmetry phase at $H < H_{cr}$ (see Fig. 1(b)). In the field along the hard axis c, the minimum on $\lambda_{12}^{\alpha}(T)$ is correlated with the transition from the low-symmetry phase (M is not parallel to H) into the high-symmetry phase ($M \parallel H$) in the field $\mu_0 H = 1.2$ T (see Fig. 1(b)).[27] The border that separates the high-symmetry and low-symmetry phases is shown in Fig. 1(b) by the dotted curve. Thus, the magnetostriction constants λ_{12}^{α} and λ_{22}^{α} are determined by the contributions of the magnetization vector orientation relative to the axis c.

The above-mentioned data indicate the coexistence of both exchange and magnetocrystalline contributions to the forced magnetostriction. It is worth noting that the field induced volume magnetostriction in the Y_2Fe_{17} compound is higher than in other intermetallic compounds at the room temperature.[4]

B. Magnetization dependence of the forced magnetostriction according to the thermodynamic theory

The experimental data of both temperature and field dependencies of the volume magnetostriction in the Curie temperature region were explained on the basis of the Landau thermodynamic theory for the second order phase transitions.[24] For a ferromagnetic with the hard

magnetization axis along the hexagonal axis c and the easy magnetization axis in the basal plane (a, b), using two components of the order parameter is sufficient: the projection of the magnetization vector ($M_\parallel$) on the axis c and on the basal plane ($M_\perp$). It has been shown by Nikitin *et al.*[27,31] for the ferromagnetic with uniaxial anisotropy in the magnetic field H and under the applied pressure P, the thermodynamic potential G can be written as

$$G = \frac{a_1}{2}m_\perp^2 + \frac{a_2}{2}m_\parallel^2 + \frac{b_1}{4}m_\perp^4 + \frac{e}{2}m_\perp^2 m_\parallel^2 + \frac{b_2}{4}m_\parallel^4 + \frac{g}{2}p^2 - \vec{m}\vec{H}, \tag{8}$$

where $m = M/M_0$ is relative magnetization, M is spontaneous magnetization at temperature T, M_0 is spontaneous magnetization at 0 K, and a_1, a_2, b_1, b_2, and e are thermodynamic coefficients. According to the theory,[27,31] we receive

$$\begin{aligned} a_1 &= a_{1\Theta}(T - \Theta^{(1)}) + \varkappa_1 P, \\ a_2 &= a_{2\Theta}(T - \Theta^{(2)}) + \varkappa_2 P, \\ b_1 &= b_{1\Theta} + \xi_1 P, \\ b_2 &= b_{2\Theta} + \xi_2 P, \\ e &= e_\Theta + \xi_3 P, \end{aligned} \tag{9}$$

where $\varkappa_1$, $\varkappa_2$, ξ_1, ξ_2, and ξ_3 are magnetoelastic coefficients and $a_{1\Theta}$, $a_{2\Theta}$, $b_{1\Theta}$, $b_{2\Theta}$, and e_Θ are thermodynamic coefficients at $P = 0$. The stable phases and the limits of their existence can be achieved from the minimization of the thermodynamic potential.[27]

In the presence of external pressure, the thermodynamic coefficients a_1 and a_2 have zero values at the corresponding temperatures $\Theta^{(1)}(P)$ and $\Theta^{(2)}(P)$, where $\Theta^{(1)}(P) = \Theta^{(1)}(0) - \varkappa_1 \frac{P}{a_{1\Theta}}$ and $\Theta^{(2)}(P) = \Theta^{(2)}(0) - \varkappa_2 \frac{P}{a_{2\Theta}}$. The volume change ω can be found directly from the thermodynamic potential (8)

$$\omega = \frac{\partial G}{\partial P} = gP + \frac{\varkappa_1}{2}m_\perp^2 + \frac{\varkappa_2}{2}m_\parallel^2 + \frac{\xi_1}{4}m_\perp^4 + \frac{\xi_3}{2}m_\perp^2 m_\parallel^2 + \frac{\xi_2}{4}m_\parallel^4. \tag{10}$$

When the applied magnetic field exceeds the magnetic anisotropy field, the magnetization vector is aligned to the magnetic field and the high-symmetry phase appears.[27]

Now let us consider three different states of a ferromagnetic in the high-symmetry phase:

(1) $H = 0$, $m_\parallel = 0$, and $m_\perp = m_S$; in this case, the spontaneous magnetostrictive deformation is

$$\omega_S = gP + \frac{\varkappa_1}{2}m_S^2 + \frac{\xi_1}{4}m_S^4. \tag{11}$$

(2) In field along easy magnetization axis ($H \perp c$), the magnetization vector is aligned to field direction ($m_\parallel = 0$) and the volume magnetostriction ω_a in the high-symmetry phase equals

$$\omega_a = \omega_\perp(H) - \omega_S(0) = \frac{\varkappa_1}{2}\left(m_\perp^2 - m_S^2\right) + \frac{\xi_1}{4}\left(m_\perp^4 - m_S^4\right), \tag{12}$$

where $\omega_\perp(H)$ is magnetostrictive deformation at $H \perp c$.

(3) For the field $H \parallel c$ (along the hard axis), the field induced volume magnetostriction ω_c in the high symmetry magnetic phase ($m_\perp = 0$) is equals to

$$\omega_c = \omega_\parallel(H) - \omega_S(0) = \frac{\varkappa_2}{2}m_\parallel^2 + \frac{\xi_2}{4}m_\parallel^4 - \frac{\varkappa_1}{2}m_S^2 - \frac{\xi_1}{4}m_S^4, \tag{13}$$

where $\omega_\parallel(H)$ is magnetostrictive deformation for $H \parallel c$. It should be noticed that change of both $\omega_\perp(H) - \omega_S(0)$ and $\omega_\parallel(H) - \omega_S(0)$ are the effects induced by the external magnetic field.

The case when $H \perp c$ (the field applied along the easy axis) corresponds to the forced magnetization as spin fluctuations close to T_C is suppressed by the magnetic field. In case when the field is applied along the hard axis ($H \parallel c$) in the low symmetry phase where $m_\perp \neq 0$, $m_\parallel \neq 0$, the process of magnetization at the phase transition is more complicated: with addition to the forced magnetization, the magnetization vector sequentially turns towards the direction of the hard axis, and at the same time the stimulation of the transverse spin waves is also suppressed.[4,32] The dependence of the field induced volume magnetostriction ω_a on the square of magnetization m^2 at the temperatures near T_C is shown in Fig. 8. It should be noticed that the thermodynamic theory (12) is well confirmed subject to the terms proportional to the squared magnetization $m_\perp^2$. Thus, the contributions to the field induced volume magnetostriction proportional to the fourth power of the relative magnetization are insignificant. According to the relation (12), the segments cut off by the straight lines $\omega_a = f(m_\perp^2)$ on the $m_\perp$ axis provide the value of the squared spontaneous relative magnetization m_S^2, and the segment cut off on the ordinate axis provide the value of the spontaneous volume magnetostriction with the minus. The experimental data for ω_a and $m_\perp^2$ allow to determine the thermodynamic coefficient $\varkappa_1 = 4.8 \times 10^{-3}$ in Eq. (12).

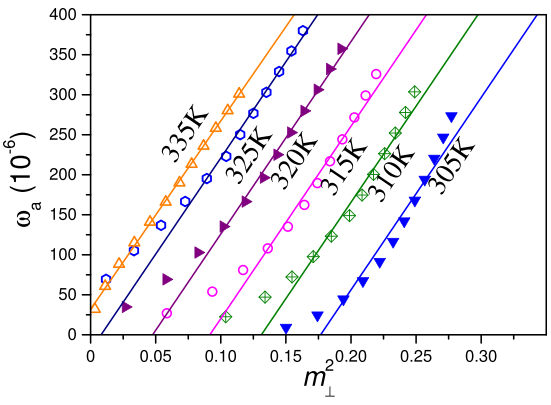

FIG. 8. The field induced volume magnetostriction ω_a versus the square of relative magnetization $m_\perp$.

C. Exchange integral dependence on the cell volume

The giant forced magnetostriction and the sharp anomalies of thermal expansion below T_C in Y_2Fe_{17} indicate the strong dependence of the exchange integral on the unit cell volume V and the interatomic distances in the Y_2Fe_{17} compound. To determine the dependence of the exchange integral (A) on the volume of the unit cell in terms of quantity, this dependence was calculated on the basis of thermodynamic correlations. These correlations suggest that the forced magnetization is the function of the T/T_C ratio and the magnetic field H. The widely known thermodynamic relation[1,4] was used for this purpose:

$$\left(\frac{\partial\omega}{\partial H}\right)_P = -\left(\frac{\partial M}{\partial P}\right)_H. \tag{14}$$

As M is the function of T/T_C and H, the following equation was obtained:

$$\left(\frac{\partial M}{\partial P}\right)_H = -T\left(\frac{\partial M}{\partial T}\right)_H \frac{\partial \ln(T_C)}{\partial P}. \tag{15}$$

It is known that compressibility k equals

$$k = -\frac{\Delta V/V}{P}. \tag{16}$$

Therefore,

$$\frac{\partial \ln T_C}{\partial P} = -\frac{k}{T_C}\frac{\partial T_C}{\partial \ln V} = -k\frac{\partial \ln T_C}{\partial \ln V}. \tag{17}$$

So, at $T = T_C$ follows from Eqs. (14)–(17),

$$\Gamma = \frac{\partial \ln T_C}{\partial \ln V} = -\frac{1}{kT_C\left(\frac{\partial M}{\partial T}\right)_H}\left(\frac{\partial\omega}{\partial H}\right)_P. \tag{18}$$

According to the experimental data in the field higher than the field of technical magnetization where the forced magnetization occurs, we obtain: $d\omega/dH = 2.5\times10^{-3}$ m/kA and $dM/dT = -10^{-3}$ T/K for the field of 1 T. The compressibility of Y_2Fe_{17} is $k = 1.05\times10^{-11}$ Pa^{-1}.[33] The exchange integral variation with the change of the unit cell volume was found by (18). According to the fact that T_C is proportional to the exchange integral A between the Fe atoms, it follows:

$$\Gamma = \frac{d\ln A}{d\ln V} = \frac{d\ln T_C}{d\ln V}. \tag{19}$$

It was found that for Y_2Fe_{17} $\Gamma = 9.1$, which correlates with the values of Γ for R_2Fe_{17} that were published by different authors in the past.[35] For example, Radwanski in his work[23] estimated this parameter as $\Gamma = 15$ using relative differences in the volumes dV of crystal lattices and the difference in the Curie temperatures dT_C in Y_2Fe_{17} and Lu_2Fe_{17} compounds. Buschow[36] estimated the value of $\Gamma = 12$ for the polycrystalline sample Y_2Fe_{17} investigating the Curie temperature dependency from lattice parameters under pressure. Givord[10] found the value of $dT_C/d\ln V = 2030$ K for the polycrystalline sample Y_2Fe_{17}, which corresponds to $\Gamma = 6.3$, from thermal expansion data (neutron diffraction).

The analysis of previously published works on the value of Γ revealed a spread in the values of Γ for R_2Fe_{17}. This may be related to two factors: (1) most of the works used polycrystalline samples and (2) different methods were used to estimate the parameter. We used single crystal samples, which allowed us to obtain a more precise value of Γ. Nevertheless, we can conclude that the exchange integral change at the unit cell volume change is extremely high in R_2Fe_{17}.

Similarly to this, the field induced volume magnetostriction in Y_2Fe_{17} reaches high values. Therefore, our investigation shows that Y_2Fe_{17} is a material with a giant field induced volume magnetostriction in moderate magnetic fields ($\omega_a \approx 360\times10^{-6}$ in the field of 1.2 T) at the Curie temperature $T_C = 324$ K (in the room temperature region). The mentioned magnetostriction is caused by the forced magnetization near the Curie temperature. This property was explained[3,19,23] by existence of abrupt change of the exchange integral between Fe atoms in 4f positions that form dumbbell-like pairs perpendicular to the hexagon composed of the nearest Fe atoms in the positions 12j. These interactions turn to be negative,[3,19,23] when the distance between two Fe atoms in the positions 4f less than critical value. According to the theory of the forced magnetostriction,[4,20] the anisotropic single-electron jumps occur in Y_2Fe_{17} in "dumbbells" of the Fe atoms in the positions 4f. These "jumps" are very sensitive to the both distances between the Fe atoms and unit cell volume. As a result of this process,[4,20] one may observe a strong dependence of the Hubbard matrix of the "jumps" t_{Fe-Fe} on deformation for 3d-electrons together with the strong decrease of the Coulomb electron repulsion (U) which leads to the giant forced magnetostriction in Y_2Fe_{17}.

Huge magnetostrictive deformations that exist in a number of materials in the low temperature region abruptly decrease together with increasing temperature. These deformations are caused by magnetocrystalline interactions. The large field induced volume magnetostriction at the Curie temperature (near room temperatures) is observed in the following materials Gd ($\omega \approx 300\times10^{-6}$)[4,34] and Lu_2Fe_{17} ($\omega \approx 150\times10^{-6}$)[4,21] in the field of 1.2 T. Therefore, the investigated Y_2Fe_{17} compound has a giant field induced volume magnetostriction that exceeds the magnetostriction in the above-mentioned materials in the room temperature region, allowing technical application of this compound. This volume magnetostriction arises from the sharp dependence of the exchange interaction. The advantage of the Y_2Fe_{17} compound is its lower cost compared with rare-earth intermetallic alloys (such as Terfenol-D) due to the high content of Fe, which is important for the technical application in magnetostrictors.

V. CONCLUSIONS

The giant field induced volume magnetostriction exists in the Y_2Fe_{17} compound in the temperature range of ferromagnetic-paramagnetic phase transition. The values of the magnetostriction constants and their temperature dependencies are explained by the Standard Magnetostriction

Theory[4] and the thermodynamic theory, where the strong dependence of the exchange interactions and magnetocrystalline interactions on the deformations should be taken into account. It was shown that the volume change at the forced magnetization in a field had anisotropic character close to the Curie temperature.

It was found that the peculiarities of the magnetostriction temperature dependence in a field applied along the hard magnetization axis were caused by the fact that in addition to the positive contribution due to the forced magnetization, the contribution from the magnetization vector rotation also existed in the fields lower than the effective field of the magnetic anisotropy. The calculated values of the magnetostriction constants λ_{11}^{α} and λ_{12}^{α} show that the anisotropic single-ion contribution and isotropic pair exchange interactions contribution are comparable in the magnitude, but the exchange contribution to the magnetostriction dominates at the Curie temperature.

The origin of the giant values of the field induced volume magnetostriction is explained by the strong dependence of the electron "jumps" parameter and the width of the 3d-electron energy band on the deformation. Special attention should be paid to the fact that the Y_2Fe_{17} compound shows the giant values of the field induced volume magnetostriction in moderate magnetic fields at the room temperature allowing using this effect in new hydraulic devices.[37]

ACKNOWLEDGMENTS

The work was supported by RFBR Grant Nos. 13-02-00916 and 12-02-31516.

[1]K. P. Belov, *Magnetic Transitions* (Consultants Bureau, New York, 1961), p. 416.
[2]K. Kulakowski and A. del Moral, Phys. Rev. B **50**, 234 (1994).
[3]K. Kulakowski and A. del Moral, Phys. Rev. B **52**, 15943 (1995).
[4]A. del Moral, *Handbook of Magnetostriction and Magnetostrictive Materials* (Del Moral Publisher S.L., Spain, 2008).
[5]V. Bodriakov, T. Ivanova, S. Nikitin, and I. Tereshina, J. Alloys Compd. **259**, 265 (1997).
[6]A. E. Clark, "Magnetostrictive RFe_2 intermetallic compounds," in *Alloys and Intermetallics*, Handbook on the Physics and Chemistry of Rare Earths Vol. 2, edited by K. A. Gschneidner, Jr. and L. Eyring (North-Holand Publishing Company, 1979), Chap. 15, pp. 231–258.
[7]K. P. Belov, G. I. Kataev, R. Z. Levitin, S. A. Nikitin, and V. I. Sokolov, Sov. Phys.-Usp. **26**, 518 (1983).
[8]M. D. Kuz'min, Phys. Rev. B **46**, 8219 (1992).
[9]F. R. de Boer and K. H. J. Buschow, J. Alloys Compd. **258**, 1 (1997).
[10]D. Givord and R. Lemaire, IEEE Trans. Magn. **10**, 109 (1974).
[11]S. A. Nikitin, A. M. Tishin, M. D. Kuz'min, and Y. I. Spichkin, Phys. Lett. A **153**, 155 (1991).
[12]O. Prokhnenko, J. Kamara, K. Proke, Z. Arnold, and A. V. Andreev, Phys. Rev. Lett. **94**, 107201 (2005).
[13]D. Gignoux, D. Givord, F. Givord, and R. Lemaire, J. Magn. Magn. Mater. **10**, 288 (1979).
[14]R. J. Radwanski, J. J. M. Franse, and K. Krop, Physica B **149**, 306 (1988).
[15]A. V. Andreev, F. R. de Boer, T. H. Jacobs, and K. H. J. Buschow, Phys. B **175**, 361 (1991).
[16]A. V. Andreev and S. Danis, J. Magn. Magn. Mater. **320**, e168 (2008).
[17]A. S. Andreenko, S. A. Nikitin, and Y. S. Spichkin, Phys. Solid State **37**, 897 (1995).
[18]A. S. Andreenko and S. A. Nikitin, Phys.-Usp. (Engl. Transl.) **40**, 581 (1997).
[19]D. Givord and E. du Tremolet de Lacheisserie, IEEE Trans. Magn. **12**, 31 (1976).
[20]A. del Moral, C. Abad, and B. Garcia-Landa, Phys. Rev. B **61**, 6879 (2000).
[21]S. A. Nikitin, I. S. Tereshina, N. Y. Pankratov, E. A. Tereshina, Y. V. Skourski, K. P. Skokov, and Y. G. Pastushenkov, Phys. Solid State **43**, 1720 (2001).
[22]K. H. J. Buschow, J. Less-Common Met. **11**, 204 (1966).
[23]R. J. Radwanski, J. Phys. F: Met. Phys. **15**, 459 (1985).
[24]L. D. Landau and E. M. Lifshitz, *Course of Theoretical Physics* (Pergamon, Oxford, 1978).
[25]T. Beuerle, P. Braun, and M. Fahnle, J. Magn. Magn. Mater. **94**, L11 (1991).
[26]K. N. R. Taylor and M. I. Darby, *Physics of Rare Earth Solids* (Chapman and Hall, London, 1972).
[27]S. A. Nikitin, A. S. Andreenko, A. K. Zvezdin, and A. F. Popkov, Sov. Phys. JETP (Engl. Transl.) **49**, 1090 (1979).
[28]E. Callen and H. B. Callen, Phys. Rev. **139**, A455 (1965).
[29]A. E. Clark, B. F. DeSavage, and E. R. Callen, J. Appl. Phys. **35**, 1028 (1964).
[30]A. E. Clark, B. F. DeSavage, and R. Bozorth, Phys. Rev. **138**, A216 (1965).
[31]S. A. Nikitin and R. V. Bezdushnyi, Sov. Phys. JETP (Engl. Transl.) **66**, 1058 (1987).
[32]K. P. Belov, *Magnetostriction Phenomena and Their Technical Applications* (Nauka, Moscow, 1987), p. 159 (in Russian).
[33]O. Mikulina, J. Kamarad, Z. Arnold, B. Garcia-Landa, P. Algabriel, and M. Ibara, J. Magn. Magn. Mater. **196–197**, 649 (1999).
[34]K. P. Belov, M. A. Belyanchikova, R. Z. Levitin, and S. A. Nikitin, *Rare-Earth Ferromagnets and Antiferromagnets* (Nauka, Moscow, 1965).
[35]R. J. Radwanski and K. Krop, Physica B+C **119**(1–2), 180 (1983).
[36]K. H. J. Buschow, M. Brouha, J. W. M. Biesterbos, and A. G. Dirks, Physica B+C **91**, 261 (1977).
[37]G. Engdahl and C. B. Bright, "Device application examples," in *Handbook of Giant Magnetostrictive Materials* (Academic Press, San Diego, 2000), Chap. 5, pp. 287–322.